Clinical Investigative Study

Similar Circuits but Different Connectivity Patterns Between The Cerebellum, Basal Ganglia, and Supplementary Motor Area In Early Parkinson's Disease Patients and Controls During Predictive Motor Timing

Ivica Husárová, MD, Michal Mikl, MSc, PhD, Ovidiu V. Lungu, PhD, Radek Mareček, MSc, Jiří Vaníček, MD, PhD, Martin Bareš, MD, PhD

From the Faculty of Medicine, First Department of Neurology, St. Anne's Teaching Hospital, Masaryk University, Brno, Czech Republic (IH, MB); Central European Institute of Technology, CEITEC MU, Molecular and Functional Imaging Research Group, Masaryk University, Brno, Czech Republic (MM, RM); Psychiatry Department, Université de Montréal, Montréal, Québec, Canada (OVL); Functional Neuroimaging Unit, Research Center of the Geriatric Institute affiliated with the Université de Montréal, Montréal, Québec, Canada (OVL); Department of Research, Donald Berman Maimonides Geriatric Centre, Montréal, Québec, Canada (OVL); Department of Radiology, St. Anne's Teaching Hospital, Faculty of Medicine Masaryk University, Brno, Czech Republic (JV); ICRC – International Clinical Research Center, St. Anne's Hospital Brno, Brno, Czech Republic (JV); Central European Institute of Technology, CEITEC MU, Behavioral and Social Neuroscience Research Group, Masaryk University, Brno, Czech Republic (MB).

ABSTRACT

BACKGROUND AND PURPOSE

The cerebellum, basal ganglia (BG), and other cortical regions, such as supplementary motor area (SMA) have emerged as important structures dealing with various aspects of timing, yet the modulation of functional connectivity between them during motor timing tasks remains unexplored.

METHODS

We used dynamic causal modeling to investigate the differences in effective connectivity (EC) between these regions and its modulation by behavioral outcome during a motor timing prediction task in a group of 16 patients with early Parkinson's disease (PD) and 17 healthy controls. Behavioral events (hits and errors) constituted the driving input connected to the cerebellum, and the modulation in connectivity was assessed relative to the hit condition (successful interception of target).

RESULTS

The driving input elicited response in the target area, while modulatory input changed the specific connection strength. The neuroimaging data revealed similar structure of intrinsic connectivity in both groups with unidirectional connections from cerebellum to both sides of the BG, from BG to the SMA, and then from SMA to the cerebellum. However, the type of intrinsic connection was different between two groups. In the PD group, the connection between the SMA and cerebellum was inhibitory in comparison to the HC group, where the connection was activated. Furthermore, the modulation of connectivity by the performance in the task was different between the two groups, with decreased connectivity between the cerebellum and left BG and SMA and a more pronounced symmetry of these connections in controls. In the same time, there was an increased EC between the cerebellum and both sides of BG with more pronounced asymmetry (stronger connection with left BG) in patients. In addition, in the PD group the modulatory input strengthened inhibitory connectivity between the SMA and the cerebellum, while in the HC group the excitatory connection was slightly strengthened.

CONCLUSIONS

Our findings indicate that although early PD subjects and controls use similar functional circuits to maintain a successful outcome in predictive motor timing behavior, the type and strength of EC and its modulation by behavioral performance differ between these two groups. These functional differences might represent the first step of cortical reorganization aimed at maintaining a normal performance in the brain affected by early Parkinson's disease and may have implications for the neuro-rehabilitation field.

Keywords: Basal ganglia, cerebellum, connectivity, supplementary motor area, cortical reorganization, Parkinson's disease, motor timing, prediction.

Acceptance: Received August 27, 2012, and in revised form March 10, 2013. Accepted for publication March 31, 2013.

Correspondence: Address correspondence to Martin Bareš, MD, PhD, Central European Institute of Technology-CEITEC MU, Masaryk University, University Campus Bohunice, Building A4, Brno, Czech Republic. E-mail: bares@muni.cz.

J Neuroimaging 2013;00:1-11.
DOI: 10.1111/jon.12030

Introduction

In the past 15 years, there has been an increasing interest in the investigation of neural correlates of temporal information processing.[1-4] Temporal computations may be distributed throughout the brain, but the evidence suggests specific roles for different neural structures. For instance, it has been proposed that the timing of short millisecond-range intervals involves the cerebellum, and that the timing of longer, second-range intervals relies on the basal ganglia (BG), with the cortical structures, such as the supplementary motor area (SMA) and prefrontal cortex being recruited in supra-second timing tasks.[1,5,6] Among these structures, the SMA was found to be important in self-initiated or "willed" actions. Increased SMA activation is thought to reflect demands on conscious temporal processing and response initiation strategies.[7,8] At the other end of the spectrum, for smaller time intervals and less conscious temporal processing, the cerebellum is believed to be involved in integrating sensory information and constructing predictions and predictive control commands that can be further processed by the cerebral cortex.[9]

In addition to the motor areas traditionally believed to be involved in processing temporal information when a motor response is required, there is recent evidence that other brain regions may also play a role in these cases. Among these other regions, the striatum occupies a central place, as it has been shown that patients with Parkinson's disease (PD) have marked deficits in motor and perceptual timing.[10–13] There are also anatomical findings suggesting that the BG, including the striatum, have extensive connections with the cerebellum.[14] Hoshi et al proposed the existence of a projection from the cerebellum to the putamen (disynaptically via the thalamus), as well as a return connection, probably via the globus pallidus, cortex, and pons. These results indicate that the BG do not play an isolated role in motor timing, but are rather part of a larger network that includes the traditional motor timing regions such as the cerebellum. In this context, it is important to elucidate the specific role of the BG in processing temporal information when a motor response is required and to what extent the functional and/or effective connectivity (EC) between the BG and other areas in this network is modulated during motor timing.

The goal of the current study is to investigate the EC between the SMA, striatum, and cerebellum and its modulation during the execution of a motor timing task. We examined this phenomenon in healthy individuals and in patients with early PD, given that this particular clinical sample is known for impairment in BG functioning, which may affect connections with other brain regions. Based on the conventional analysis of fMRI data collected during an interception task in a previous study,[15] we selected four regions of interest (ROIs) for the current analysis using dynamic causal models (DCMs): left and right putamen, SMA, and right posterior cerebellum. In the current study we expanded the traditional analysis of the previous data by using DCMs and investigating the differences in connectivity between these regions and its modulation by behavioral performance in the two groups.

Given the evidence that the cerebellum and BG are jointly involved in motor timing, we hypothesize that we will find differences between HC and PD subjects either in their ability to postpone their motor responses or in an increased likelihood of producing an error when the prediction timing interval is long. Also, given the involvement of the BG in processing the error signal in prediction tasks,[16,17] we expected that PD subjects might show a reduced adaptation of their motor responses after an error, relative to HC. In terms of imaging results, we expected to observe changes in the EC in the network comprising these structures, as well as their cortical projections both as a function of task performance and as a function of having or not a perturbation induced by the disease (ie, PD vs. HC).

Methods

Subjects

Our study included 16 patients with idiopathic early-stage Parkinson's disease (PD group) and 17 healthy volunteers (HC group). The patients were diagnosed according to the United Kingdom PD Brain Bank Criteria.[18] The accuracy of the PD diagnosis was proved by subsequent long-term clinical follow-up. The PD subjects were scored according to the Unified Parkinson's Disease Rating Scale (UPDRS),[19] with a mean UPDRS score in the "off" state of 18.08, SD ±3.8. The PD group had 9 men and 7 women, with a mean age of 55.3, SD ± 8.7 years; the mean length of illness was 2.5 years. At the onset of illness, 12 subjects had unilateral right parkinsonian symptomatology and four subjects had unilateral left symptomatology. All of the PD patients had mild bradykinesia and hypokinesia. Of the 16 PD patients, 10 received D2 agonists (ropinirole 4 patients, mean dose 15 mg; pramipexole 6 patients, mean dose 2.3 mg); none of them received L-DOPA medication; 6 PD patients were drug-naive. The fMRI experiment took place in the "off" state (subjects were off medication for at least 16 hours). The results of the modified Minnesota Impulse Disorders Interview did not reveal any signs of impulsivity. None of the subjects in the study were depressed according to the diagnostic questionnaire, which included the Montgomery-Asberg Depression Rating Scale (MADRS). Two tests of cognitive function, the Mini-Mental State Examination (MMSE) and Montreal Cognitive Assessment (MoCA), revealed no cognitive impairment. None of the subjects had dementia. More detailed clinical data and neuropsychological testing were published in our previous study.[15]

The control group consisted of 17 healthy volunteers with no symptoms of neurologic diseases (9 men and 8 women; mean age 57.0, SD ± 7.3). All subjects in both groups were right-handed according to the Edinburgh Handedness Inventory.[20] PD group nor healthy group reported any visual problems. Standard neurological examination did not reveal any anormalities related to the visual system abnormalities. The data from classical fMRI analysis pertaining to these participants were presented in a previous, larger study.[15] All the subjects gave their informed consent before participating in the experiment. The study was approved by the Institutional Review Board of St. Anne's Hospital, Brno.

The Interception Task

We used the same interception task requiring motor timing (ie, accurate perception of target temporal information and a

precise, timed motor response) as that employed before with patients with spinocerebellar ataxia, essential tremor, and early PD.[21,22] The task was programmed using Lab VIEW 6.1™ (National Instruments, Austin, TX, USA).

The participants were asked to press a button with the right finger in order to intercept a target that moved from the left to the right side on a computer screen. There were three different types of target movement: constant, decelerated, and accelerated. The target was a green ball that moved across the screen at three different speeds (slow, medium, and fast) and at three different angles (straight across, 15° angle, or 30° angle). A fireball traveled up from a blue cannon located at the lower right of the screen with a constant speed of 20 cm/second to intercept the moving target. The fireball reached the target zone in about 1.1 seconds. The diameter of the target was 1 cm; the diameter of the fireball was .3 cm. The interception zone was always in the same position on the screen: the right upper side of the screen. If the subject successfully intercepted the target, both balls exploded. If the subject failed to intercept the target, no explosion animation occurred. In order to discourage a response strategy based on counting the time from the target's appearance on the screen until the push of the button, we asked subjects not to count overtly or mentally during the whole experiment. In addition, the presentation of various types of stimuli within a block was counterbalanced to minimize the repetition of the same type of stimuli in consecutive trials.

Prior to performing the main task, subjects practiced three tasks in the scanner (with acquisition). Each practice task lasted 3 minutes. In the first practice task, there was no fireball, but a cross was displayed at the interception point. Participants were instructed to press a button when the target reached the cross. In the second practice task, participants were instructed to press a button when the target color changed from green to red. The third practice task was arranged the same way as the main task. The main task lasted approximately 19 minutes, and was divided into six blocks, each consisting of 54 stimuli (trials), separated by 20-second break periods that involved no stimulation. One break period also preceded the first block and one followed the last block. The whole main task had a total of 324 stimuli. The target (green ball) could be any combination of the three variables described earlier (type of movement, speed, and angle), giving a total of 27 separate potential target movement conditions. However, the movement type remained the same for each block (either constant, decelerating, or accelerating). Each combination of a particular trial type was presented twice (total of 54 stimuli). The movement type was selected pseudo-randomly from six preprogrammed variants. The duration of stimuli altered among 2.5, 3.0, and 3.5 seconds according to the stimulus type. For each stimulus, the subject had only one chance to press the button. The computer system did not respond to any additional pressing of the button.

A short 3-minute postpractice task followed, with instructions to press the button when the target's color changed. The duration of the whole experiment was 60 minutes (including the acquisition of anatomical scans as well as necessary delays within the MR scanner). None of the participants reported that they were tired at the end of the experiment. More extensive description of the task was provided in previously published study.[15]

Image Acquisition Parameters

Imaging was performed on a 1.5 T Siemens Symphony scanner equipped with Numaris 4 System (MRease). Functional images were acquired using a gradient echo, echoplanar imaging (EPI) sequence: TR (scan repeat time) = 2300 ms, TE = 35 ms, FOV = 220 × 180 mm, flip angle = 90°, matrix size 64 × 52, inplane voxel size = 3.438 × 3.461 mm, slice thickness = 4.4 mm, 28 transversal slices per scan. The image volume covered the whole brain, including the whole cerebellum. Each functional study consisted of three practice runs (90 volumes each), one main run (490 volumes), and one postpractice task run (90 volumes). These runs were each separated by only the few seconds needed in order to repeat the instructions for next part. The subjects were instructed to stay still during these breaks and throughout all measurements. Following functional measurements, high-resolution anatomical T1-weighted images were acquired using a 3-D sequence that served as a matrix for the functional imaging (160 sagittal slices, resolution 256 × 256, slice thickness = 1.17 mm, TR = 1700 ms, TE = 3.96 ms, FOV = 246 mm, flip angle = 15°).

Behavioral Data Analysis

We recorded the outcome (hit or miss) in each trial. In order to be able to use parametric statistical techniques (eg, generalized linear model–GLM) with this type of dichotomic data and to have a normal distribution for the hit ratios, we computed the percentage of hits for each subject and for each type of trial based on a combination of movement type, speed, and angle (a total of 27 values per block). Kolmogorov-Smirnov tests showed that this new dependent variable was distributed normally, thus allowing its use in the GLM analysis. The GLM had four independent factors (group, movement type, speed, angle) and was fully factorial, assessing all of the main effects and possible interaction effects between these factors on the percentage of hits. As such, the GLM assessed the differences in hit ratio percentages between groups, as well as the influence of movement parameters (movement type, speed, and angle) on performance. In the GLM analysis, subjects were always entered in the model as a random factor. Each "miss" trial was classified as an early or late error depending on whether the "fire" button was pressed too early or too late to achieve a hit. We then employed nonparametric tests (eg, chi-square) to test whether the two groups were significantly different in terms of the distribution of hits and early and late errors. Given that this measure tends to augment with the number of cases taken into account, we decided to rely on phi and Cramer's V coefficients, which use chi-square, but account for the sample size. Taking the distribution of these types of trials observed in healthy controls as a reference, we used phi and Cramer's V correction of the chi-square test to assess whether the PD subjects had a similar or different distribution than that of healthy controls.

Conventional Imaging Data Analysis

SPM5 program (Functional Imaging Laboratory, the Wellcome Department of Imaging Neuroscience, Institute of Neurology

at University College London, UK) running under Matlab 6.5 (Mathworks Inc., USA) was used to analyze the fMRI data. Only the data from the main task were analyzed. The following preprocessing was applied to each subject's time series of fMRI scans: realignment to correct for any motion artifacts; normalization to fit into a standard anatomical space (MNI); spatial smoothing using a Gaussian filter with a FWHM of 8 mm; high-pass filter with a cut-off at 512 seconds; and an autoregressive model (first order–AR(1)–as implemented in SPM software) to estimate serial correlations.[23] The voxel size generated from the above acquisition parameters was sampled at $3 \times 3 \times 3$ mm. Subject responses were categorized as HIT: successful interception of the moving target; EARLY ERROR: button pressed too prematurely to hit the target; LATE ERROR: button pressed too late to hit the target. To determine the brain regions that showed significantly greater time-locked activation to hits, early errors, or late errors, a GLM as implemented in SPM5 was used. Each stimulus onset was modeled from the moment the target appeared on the screen and ended when the target disappeared (for miss trials) or after the explosion animation ended (for hits). For the traditional fMRI analysis, we used a GLM model with three factors of interest describing subject responses (early errors, hits, late errors). A canonical hemodynamic response function (HRF) was selected as a basis set for analysis. Three experimental conditions were used in the analysis, convolved with the HRF: one for hits, one for early errors, and one for late errors. After estimating the parameters for the GLM model at the individual level, contrast files for each condition were subsequently used for the second-level random-effects analysis to assess the group differences (ie, between PD subjects and healthy controls). Based on behavioral results indicating that the two groups were different in terms of their early errors relative to hits, we decided to use the contrast between these two predictors for the main imaging results in order to assess the differences in the BOLD signal between the PD and HC groups. For the group results, we used a false discovery rate (FDR) threshold of .0005 with a minimal spatial extent of 25 voxels. The group activation maps are presented here, but they are not the results of interest for the current paper; instead, they serve to identify and select the ROI used for the DCM analysis.

Additionally, for both groups, we contrasted all trials (hits and errors together) against the baseline. We reasoned that this contrast would probably reveal the activity related to motor timing in general (because, regardless of the outcome, the participants will always try to predict the trajectory of the target, ie, will engage in motor timing) rather than that related to the reward, as this mixes both hits and errors.

Dynamic Causal Modeling of Imaging Data

We performed the DCM analysis[24] as implemented in SPM5 package in order to test our hypothesis about EC during an interception task. Four ROIs were selected for the DCM by using the group-level statistical parametric maps from the traditional fMRI analysis for the contrast (Hits > Early Errors). These regions include the left (PutL) and right (PutR) putamen, SMA, and right posterior cerebellum (Cer)–Crus I and lobule VI, consistently activated in all subjects (Fig 1). To account for interindividual differences in the peak locations of brain activations, individual coordinates of these ROIs were found for each subject at the nearest local maximum of the given functional region. Initial coordinates selected from group activation maps are highlighted in Table 1. Functional time series were extracted from spherical volumes (6 mm radius) and entered into the DCM. Only the time series from voxels with $P < .01$ uncorrected were used for analysis. An eigenvariate (first principal component) was calculated from these time series. This results in one time series per region, with a greater signal-to-noise ratio than a single voxel time series.

The time series were adjusted with respect to the effects of all three conditions. This means that the null space time series was subtracted from the filtered and whitened time series, and the effects of nuisance variables (for instance, mean signal intensity) were removed. The final time series variations are caused only by the experimental effect of interest. Given the established role for the cerebellum in motor timing, we decided to choose this region as the driving input for DCM analysis.[24] To verify our hypothesis about input regions, we used the same strategy as in Ethofer et al.[25] We tested four fully connected models, each with a different region used for driving input (cerebellum, SMA, and left and right putamen). All these models were then compared using the Bayesian model selection procedure.

DCM deals with two types of inputs: direct and modulatory. Direct input elicits responses in the target area, while modulatory input changes the specific connection strength. A combination of all three conditions was used as the direct input. Hits were used for modulatory inputs on all allowed interregional connections. The reason for using the hit rather than an error as a modulatory input is two-fold. We were interested in identifying the connectivity strengths when individuals were successful in performing the task, ie, when their behavior was optimal. We wanted to show how the brain activity is reorganized to obtain optimal behavior when affected by the disease. This goal is even more important in the light of behavioral results (reported in Husarova et al, 2011) which showed that a PD group could execute the task at almost the same level as the healthy controls (early PD performance was 90% that of the HC group).[15] Changes in the connectivity strengths can thus inform us of the patterns of reorganization of brain activity needed for a PD group to achieve results comparable to those of an HC group, hence providing evidence of possible compensatory mechanisms. Further, the ROIs selected for the connectivity analysis responded to a greater level of activity during hits than during early errors (results of the classical fMRI analysis) in both groups. Thus, the modulation introduced by hits will provide information on how connectivity changes within the same brain functional network as a function of the disease.

Seven possible models were created (Fig 2) and the goodness-of-fit for each was estimated. These hypothetical models and their connections were selected according to anatomical and functional interconnections among SMA, cerebellum, and BG.[26,27] One model was fully connected; the other six represented different connectivity patterns, all without a direct connection between the left and right putamen. All of these models were created for each subject. The best model over all

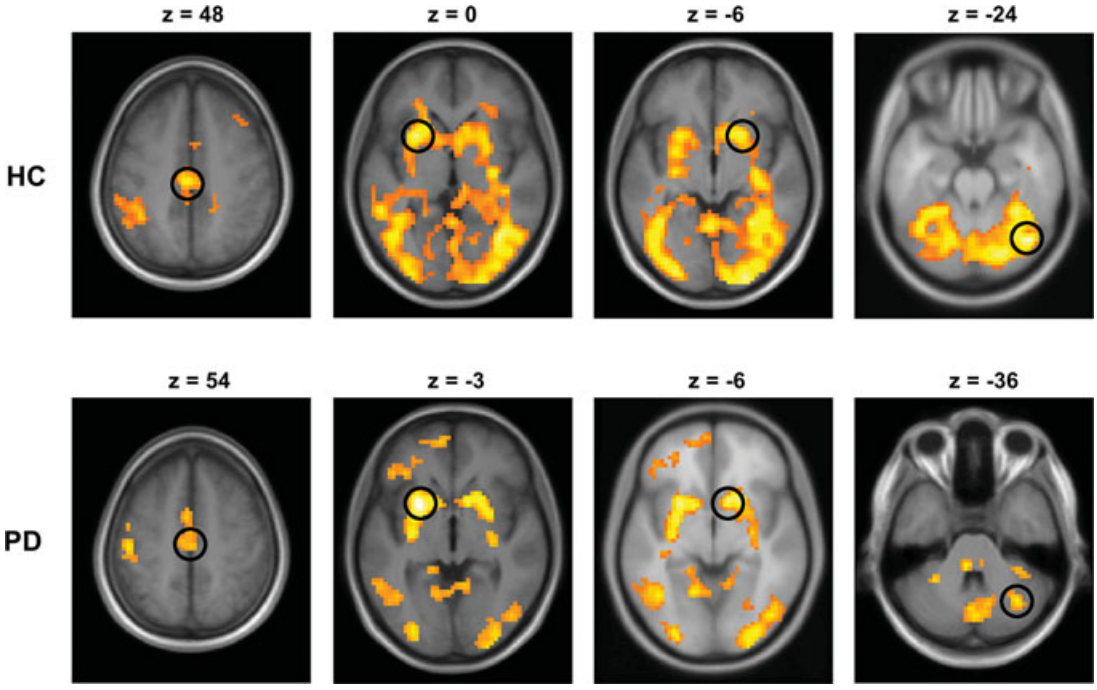

Fig 1. Composite maps of 17 healthy controls and 16 early PD subjects showing brain regions significantly activated in the interception task contrasting hits minus early errors, at a .0005 FDR level of significance. Regions of interest are indicated by black circles.

subjects (healthy controls and PD subjects) was selected using binomial probabilities as previously demonstrated.[15] Model evidence was computed based on Bayesian and Akaike's information criterion (BIC and AIC, respectively) for each subject and each pair of models. Subsequently, *P*-values were calculated for each pair of models according to the binomial distribution for the number of Bayes factors (BF) greater than one. The group Bayes factors (GBF) were calculated in the standard manner. GBF corresponds to fixed-effect analysis and is sensitive to distant values. The best model was selected for all subjects (both groups combined) and also separately for each group (PD subjects and healthy controls) to assess for possible differences in the main connectivity pattern. The same model was selected for both individual groups and for the combined data set. Only the BF for joint data selection (across all subjects) is presented in Table 2. Average parameters across each group were obtained using the built-in function in SPM5 (Bayesian averaging). The connections with posterior probabilities (strength greater than zero) greater than 90% were considered as significant. To assess the connection strength differences between the two groups, we used the random-effect approach with a two-sample *t*-test.

Results

Behavioral Results

Hit Ratio and Kinematic Parameters

The GLM analysis indicated that the PD subjects had a lower overall hit ratio than the healthy controls [41.08 ± 8.41 vs. 45.50 ± 7.29; $F_{(1,31)} = 4.47$, $P < .05$]. However, despite this overall difference in hit ratio, the two groups were similarly affected by the kinematic properties of the moving target (Supplementary Fig 1A), as indicated by the lack of significant interaction effects between the groups and the variables characterizing the target's movement (movement type, speed, and angle). For instance, we did not find any significant interaction between group and movement type [$F_{(2,62)} = 1.03$, $P = .36$], group and speed [$F_{(2,62)} = .36$, $P = .69$], group and angle [$F_{(2,62)} = 1.03$, $P = .36$], or any other combination of these variables that included the group factor (all $P > .05$). In conclusion, although the PD subjects had a hit ratio that was about 90% of that of the healthy controls, they were affected by the kinematic properties of the target to the same extent.

Trial Type Distribution

The distribution of hits and early and late errors was different between the two groups. While in both the PD and healthy groups, the hits surpassed the percentage of early or late errors (Supplementary Fig 1B; there were significantly more early errors and fewer hits in the PD group than in the control group, as revealed by both chi-square [$\chi^2 = 56.76$, df = 2, $P < .001$] and Cramer's V correction [V = .73, $P < .001$]). These results indicate that the PD subjects tended to make late errors to the same extent as the healthy controls and that the difference in hit ratio between the two groups comes from the PD subjects' tendency to make more early errors. Furthermore, the trial-by-trial analysis, presented in Supplementary materials (Fig 1C), showed that the PD group tends to press the button earlier than necessary as a strategy to adapt their behavior after an error, thus increasing the likelihood of committing an early error. This differential behavior, the tendency to press the button earlier than later, supports our timing hypothesis.

Table 1. The Activation Strength of Different Areas Thresholded at a .0005 FDR Level of Significance with Extent Threshold (minimal cluster size) of 25 voxels

Hit versus Early Errors	Area	BA/CER	Coordinate MNI	Voxel	*T*-Statistic	*Z*-Statistic
Healthy controls						
	SMA	BA 6	**–3 –24 48**	113	6.82	5.52
	Cerebellum R superior	crus I	**42 –66 –24**	342	9.46	6.82
	Putamen L		**–27 12 0**	219	8.67	6.47
	Putamen R		**21 12 –6**	186	7.68	5.99
	Cerebellum L	VI	–30 –45 –24	335	7.57	5.93
	Cerebellum R	VI	24 –75 –24	403	8.26	6.27
	Cerebellum L	IV,V	–3 –57 –6	170	7.73	6.01
	Cerebellum	vermis	0 –54 –3	98	8.03	6.16
	Temporal Inferior, fusiform gyrus L	BA 37	–51 –48 –15	165	7.81	6.05
	Temporal middle L	BA 21	–54 –45 0	166	7.61	5.95
	Parietal supperior L	BA 7	–18 –63 42	219	6.04	5.06
	Anterior prefrontal cortex L	BA 10	–33 60 9	28	5.76	4.89
	Dorsolateral prefrontal cortex R	BA 9	48 27 33	37	5.66	4.83
	Frontal inferior R	BA 47	30 30 –3	25	5.65	4.81
	Temporal gyrus R	BA 41-42	54 –18 9	38	5.50	4.72
	Precuneus Parietal lobe R	BA 7	18 –45 45	27	5.46	4.69
	Fusiform occipital gyrus R+ border of cerebellum	BA 37	33 –45 –18	473	9.06	6.64
	Fusiform occipital gyrus L	BA 37	–39 –54 –9	260	8.17	6.23
PD subjects						
	Putamen L		**–24 9 –3**	1068	9.53	6.85
	Putamen R		**12 12 –6**	517	8.03	6.16
	SMA	BA 6	**0 –21 54**	85	6.82	5.52
	Cerebellum R	V	**27 –33 –42**	54	6.00	5.04
	Temporal inferior L	BA 37	–51 –48 –15	172	9.35	6.77
	Precuneus Parietal lobe R	BA 7	21 –51 21	690	6.56	5.37
	Parietal inferior L	BA 40	–51 –42 51	830	6.43	5.29
	Frontal inferior gyrus	border of BA 9-44	–51 12 39	105	6.38	5.27
	Occipital middle L	BA 18	–30 –90 –6	68	6.29	5.22
	Occipital middle R	BA 19	33 –81 27	117	5.76	4.88
	Frontal supperior med. L	BA 10	–9 57 0	41	5.52	4.73
	Occipital inferior gyrus R and cerebellum posterior lobe	BA 19	39 –87 –12	1002	7.58	5.93

Note: Areas Marked in Black were Selected for the DCM.

Imaging Results–Conventional GLM Analysis

Given that the behavioral results showed that the two groups were different in terms of their early errors and hits, we decided to use the contrast between these two predictors in order to assess the differences in the BOLD signal between the PD and HC groups. We analyzed the BOLD signal corresponding to the contrast between early errors relative to hits in both groups, as described in the Methods section.

In both groups, we found an increased activation during hits relative to early errors bilaterally in the BG. We also observed an increased activation in the cerebellum, with maximum activity in the Crus I, in lobule VI, and the cortical areas (anterior and dorsolateral prefrontal cortex, parietal, and temporal regions, and V2/V3 cortex), including SMA at a .0005 FDR level of significance (Table 1; Fig 1). All trials (hits and errors together) revealed activation in the BG in both groups, with a stronger result in the HC group (activation was there when corrected using FWE) and a weaker result in the PD group (activation was there when we did not correct FWE). These findings reflect the involvement of this structure in motor timing, although part of the BG activity that we observe when we contrast hits with errors may be reward related.

Dynamic Causal Modeling

To verify our hypothesis about input regions, we used the same strategy as in Ethofer et al.[25] We tested four fully connected models, each with a different region used for driving input (cerebellum, SMA, and left and right putamen). All these models were compared using the Bayesian model selection procedure. The model with input into the cerebellum was identified as the best model (model exceedance probability .4797 for the cerebellum, versus .3166 for the right putamen, .1553 for the left putamen, and .0484 for SMA). The model with an input into the SMA is the least probable model.

According to the method used by Ethofer[25] and based on our hypothesis, we selected the seven hypothetical models with driving input into the cerebellum, as the most probable input. All of these models were estimated and compared. We found model 3 to be superior to the other (there was a better statistical fit with the data, and it better explained the variability of the data) and this model fits well both the PD and HC groups (Fig 3). The BFs for the combined data selection (across all subjects) are presented in Table 2. All coefficients of connections in the model have at least a 90% posterior probability ($P > .9$) of a value was greater than zero, indicating that the two nodes are

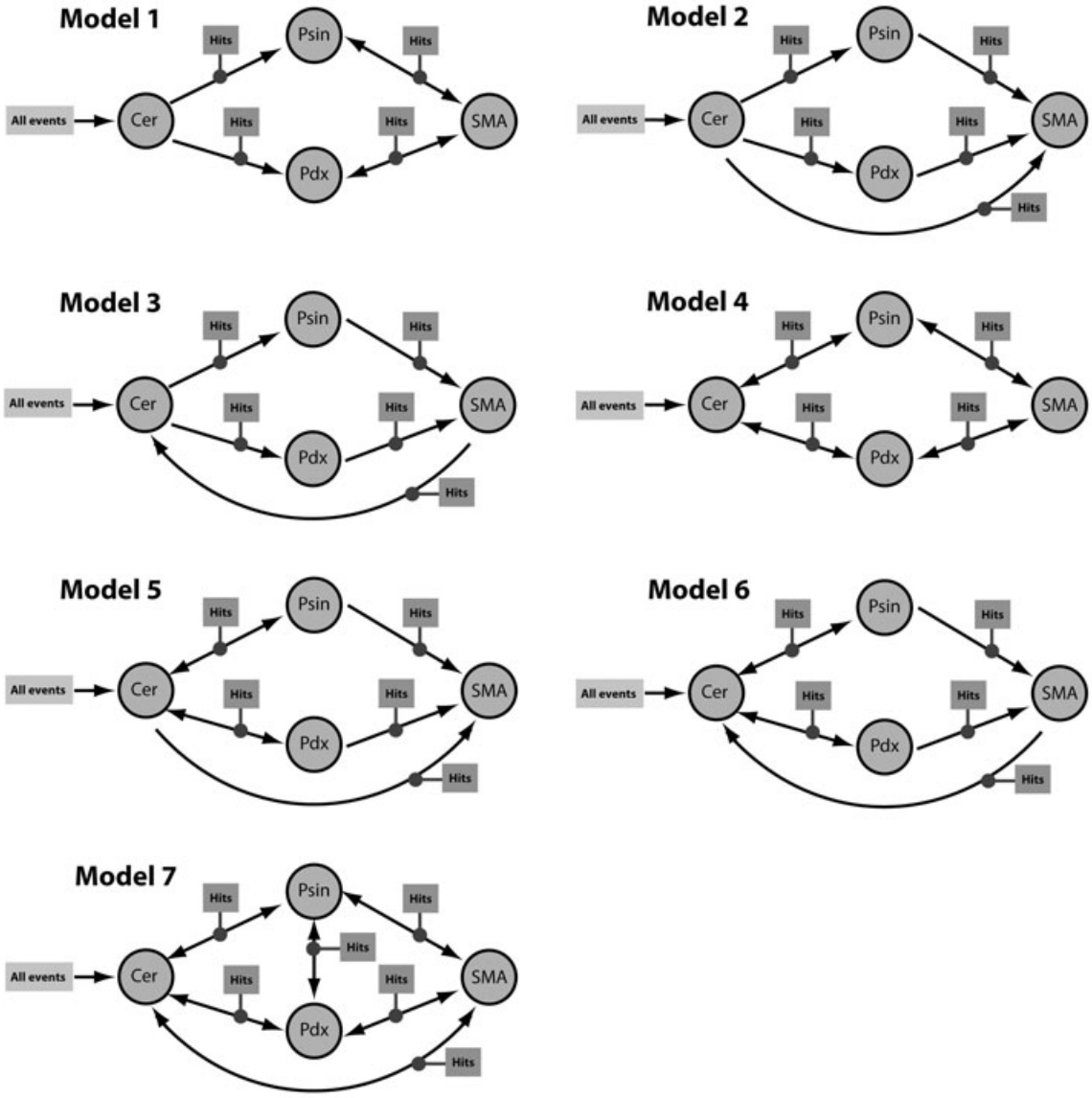

Fig 2. Hypothetical models of intrinsic connectivity structures of dynamic causal models for driving input connected in the posterior cerebellum. Intrinsic connections are shown as directed black arrows (unidirectional arrows indicate connections from a region of interest, and bidirectional arrows indicate reciprocal connections).

connected or exchange information in more than 90% of the cases. Thus, even a small magnitude of the connection plays an important role in the model (for a specific connection) although we cannot decide whether very small value is physiologically (biologically) sensible. This is a limitation of interpretation of some of our results, eg, modulatory change of connection from SMA to the cerebellum in the control group. The structure of intrinsic connectivity in both groups showed that the posterior cerebellum has unidirectional connections with both the left (dominant connection) and right putamen. Unidirectional connections of the BG with the SMA and of the SMA with the cerebellum were present. In the HC group, the modulatory input decreased the connection among the cerebellum, left putamen, and SMA, with more pronounced symmetry of these connections on both sides of the BG. In contrast, the PD group showed increase in EC between the cerebellum and putamen bilaterally with more pronounced asymmetry (stronger connection with the left putamen). In the PD group, the results revealed that the connection between the SMA and cerebellum was inhibitory in comparison to the HC group, where the connection was activated. In addition, in the PD group the modulatory input strengthened inhibitory connectivity between the SMA and the cerebellum, while in the HC group the excitatory connection was slightly strengthened (Fig 3). We did not find any difference in connectivity based on whether the PD patients presented right or left dominant symptomatology.

Differences in connection strength between the PD and HC groups were assessed using *t*-tests on connection strengths of individual subjects. Regarding the magnitude of intrinsic connectivity coefficients between the network nodes, we did not find

Table 2. The Comparison of Models 1 to 7 (7 = fully connected) for all 33 Subjects (PD + healthy controls)

Model	1	2	3	4	5	6	7
1	*	$B_{12} = 1.07e20$ $P = .993$	$B_{13} = 7.36e\text{-}21$ $P > .999$	No evidence $P = .919$	No evidence $P = .500$	No evidence $P = .500$	No evidence $P = .500$
2	$B_{21} = 9.32e\text{-}21$ $P = .852$	*	$B_{23} = 5.29e\text{-}101$ $P = .993$	No evidence $P = .993$	No evidence $P = .919$	No evidence $P = .918$	No evidence $P = .919$
3	$B_{31} = 1.36e20$ $P = .040$	$B_{32} = 1.89e100$ $P = .017$	*	No evidence $P = .148$	$B_{35} = 1.83e18$ $P < .001$	$B_{36} = 3.35e16$ $P < .001$	No evidence $P = .007$
4	No evidence $P = .993$	No evidence $P = .993$	No evidence $P = .999$	*	$B_{45} = 1.13e37$ $P = .997$	$B_{46} = 2.07e35$ $P = .993$	$B_{47} = 4.45e59$ $P < .001$
5	No evidence $P = .997$	No evidence $P = .999$	$B_{53} = 5.48e\text{-}19$ $P > .999$	$B_{54} = 8.87e\text{-}38$ $P = .852$	*	$B_{56} = .018$ $P = .081$	No evidence $P = .040$
6	No evidence $P = .997$	No evidence $P = .999$	$B_{63} = 2.98e\text{-}17$ $P > .999$	$B_{64} = 4.83e\text{-}36$ $P = .500$	$B_{65} = 54.46$ $P = .960$	*	No evidence $P = .040$
7	No evidence $P = .999$	No evidence $P = .999$	No evidence $P > .999$	$B_{74} = 2.24e\text{-}60$ $P > .999$	No evidence $P > .999$	No evidence $P > .999$	*

Notes: The table is designed as follows (see also Ethofer et al., 2006): Each cell represents the comparison of one model (indicated by row number) to another one (indicated by column number). B_{xy} is the group Bayes factor representing the ratio of probability of model x versus probability of model y. P-values represent the binomial probability that individual Bayes factors are not consistent according all subjects. Significant results of model comparisons (ie, $P < .05$) are marked by gray color. Comparisons of same models (on diagonal) are irrelevant and marked by asterisk.

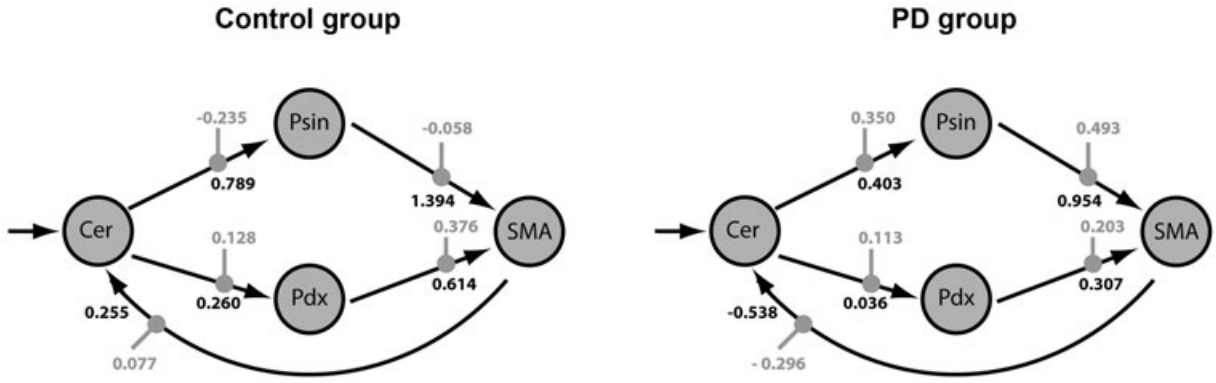

Fig 3. The most probable structure of intrinsic connectivity in PD subjects and healthy controls. Intrinsic connections are shown as directed black arrows. Significant connection strengths (averaged across individuals at 90% confidence) are reported alongside the arrows with black numbers. Modulation effects by hit condition and averaged strengths of these effects across individuals are presented with gray numbers.

any significant differences between the two groups based on two-tailed t-test. However, if one considers the direction of our hypothesis (ie, we expected a decreased connectivity among PD patients in comparison to HC), then two intrinsic connections revealed some significant trends ($P < .05$ one-tailed uncorrected for multiple testing): the connection from the right putamen to the SMA ($P = .085$ two tailed and $P = .043$ one-tailed) and the connection from the SMA to the cerebellum ($P = .062$ two-tailed and $P = .032$ one-tailed). The differences produced by the modulatory input were tested by adding the intrinsic connectivity coefficient with the modulatory input change in coefficient, which, in effect, reflects the intrinsic connectivity in the network during successful trials (hits). Again using the independent samples t-test, we found a significant difference (one-tailed and uncorrected for multiple testing) between the two groups in the connectivity between the SMA and cerebellum [$t(31) = 1.997$, $P = .05$ two-tailed or $P = .026$ one-tailed], with the intrinsic connectivity during hits being greater in the HC than in the PD group (Table 3), and difference in the connectivity between the right putamen and SMA ($P = .098$ two tailed or $P = .049$ one-tailed) also with the intrinsic connectivity during hits being greater in the HC than in the PD group.

Discussion

We investigated differences in EC patterns between early PD patients and controls in a brain network comprising cerebellum, BG, and SMA during a predictive motor timing task.[15] We suggested that the distinct behavior between the groups (the tendency to press the button earlier rather than later) supports our timing hypothesis by showing that PD patients have a perturbation of their motor response after an error, with the inability to adapt their motor timing after an error as a manifestation of the impaired functioning of the striatum. The results of conventional fMRI analysis revealed that subcortical structures, such as the putamen and cerebellum, and also cortical areas such as the SMA, the anterior and dorsolateral prefrontal cortex, the parietal and temporal regions, and the V2/V3 cortex were implicated in the predictive timing task. These findings are in agreement with the results of previous fMRI studies focused

Table 3. Comparison of Connection Strengths between the Control and PD Groups using Two Sample *t*-test

	LPut-SMA	Cer-LPut	Cer-RPut	SMA-Cer	RPut-SMA
Intrinsic connections					
P-value one tailed *t*-test	.330	.263	.216	**.032**	**.043**
P-value two tailed *t*-test	.660	.525	.432	.062	.085
Modulatory changes in connection					
P-value one tailed *t*-test	.064	.413	.424	.077	.121
P-value two tailed *t*-test	.127	.825	.848	.154	.241
Connection after HITs					
P-value one tailed *t*-test	.453	.340	.255	**.026**	**.049**
P-value two tailed *t*-test	.905	.680	.510	.0547	.098

Note: Significant results, uncorrected for multiple testing, (ie, $P < .05$) are in bold numbers. LPut = Left Putamen; RPut = Right Putamen; Cer = Cerebellum; SMA = Supplementary Motor Area.

on temporal processing and visuospatial orienting.[6,28,29] While the activations of the BG and the cerebellum indicated that these regions are involved in motor timing regardless of the outcome in each trial, four brain regions were found to be involved in timing prediction (putamen bilaterally, SMA, and right cerebellum), reflecting a combination of both better motor timing and reward processing. These regions were selected for the DCM analysis, which showed that early PD subjects and controls use similar functional circuits to achieve successful outcomes in predictive motor timing behavior.

The cerebellum was chosen as a region for driving input for DCM and our Bayesian model selection procedure confirmed this choice. This hypothesis was built on previous anatomical findings[14] and evidence suggesting that the cerebellum is responsible for constructing sensory predictions and predictive control commands that can be further processed by the cerebral cortex.[9] Relevant empirical literature suggests that the SMA plays a key role in time processing as part of the striatocortical pathway, previously identified in animal studies, human neuropsychology, and neuroimaging.[30] For instance, in past studies, Akkal et al used retrograde transneuronal transport of neurotropic viruses to define the organization of the BG and cerebellar projections to the SMA. They found that the SMA are the targets of outputs from both the BG and the cerebellum, but that the SMA receives relatively more input from the BG than the cerebellum.[26] Disynaptic projection from the cerebellum to the BG and a reciprocal projection from the BG to the cerebellum was also described.[31] Although we found that the PD subjects and controls used similar functional circuits to fulfill the task demands, the type of intrinsic connection (inhibitory vs. excitatory between SMA and cerebellum) was different between the groups. Furthermore, the modulation within these functional circuits and the strength of EC was found to differ between these two groups considering the modulatory input during successful trials. One limitation of our results with respect to the average group connection strengths (calculated with Bayesian averaging, presented in Fig 3) is that very small values of modulatory effect were interpreted (specifically the value .077 between SMA and cerebellum in the HC).

Although we have at least 90% probability that this value is greater than zero and therefore it is important for estimated model, we are not able to determine whether such small effect is biologically plausible. The other limitation is related to the between-group comparison calculated using the random-effect approach with two-sample *t*-test based on individual connection strengths. Results are significant at uncorrected level (without correction for multiple testing). Thus, the interpretations need to be made with caution. On the other hand, we believe that the difference between the HC and PD groups related to the connectivity between SMA and cerebellum is important. It points out to the different types of connection (inhibitory vs. excitatory) as was revealed with Bayesian averaging (see Fig 3).

EC describes networks of directional effects of one neural network over another, where changes in activity in one network can precede similar changes in activity in another network, with the inference that the first network is causally influencing the activity in the second network. As such, positive changes in EC indicate that an increase in activity in the first network will be followed by an increase in activity in the second network, with negative coefficients indicating the reverse. Physiologically, a positive EC could be seen as one network exerting an excitatory effect over the second network, and a negative EC could be conceived as an inhibitory influence. In this context, our EC model revealed that the cortico-cerebellar excitatory connection (from the SMA to the cerebellum) seems to be reinforced in an HC group during hits as compared to PD patients. Granger causality methods measured evidence for the existence of a strong and positive EC between the SMA and right cerebellum in healthy individuals,[32] which is in line with our results. Given that PD patients are able to perform the task at a level comparable to that of the HC individuals (90% of the healthy controls performance), one can interpret the reduction in connectivity during hits between the SMA and cerebellum as a form of compensatory mechanism, maybe even inhibitory in nature. There is indirect evidence from a deep-brain stimulation study describing that while SMA activity decreased, the cerebellar activity increased as a function of subthalamic nucleus stimulation and increased task performance.[33] We believe that these results, as well as ours, point to a compensatory mechanism in PD patients, whereby successful execution of a motor task is associated with an inhibitory or a reduced connection between the SMA and cerebellum. Further, in the PD group, we found a stronger connection between the right cerebellum and the left putamen after the modulation input. This connectivity pattern was the same in the early PD

patients with dominant right-sided or left-sided parkinsonian symptomatology. Early PD patients during the experiment continued to be asymmetric. Our results indicate that parkinsonian motor (side) asymmetry and the associated contralateral impairment of BG do not influence the motor timing and time data processing in BG. This finding is in concordance with the results of our previous work[15] where we observed no effects of the lateralization of PD symptomatology on the behavioral or imaging data. Overall the ability of early PD patients to execute the task at almost same level as the HC group is consistent with the results of studies suggesting a lack of impairment in perceptual timing in early stage PD,[34] and the correlation of timing deficits with disease severity.[7,35]

It would be equally interesting to investigate the role of other areas (prefrontal and parietal areas) activated during an interception task. Our method is hypothesis driven rather than data based,[24,36] which is one of the limitations of DCM and all other methods of analyzing EC. This method specifies the model of interaction and the results are closely bound with the model. We believed that it was therefore essential to select regions that are unambiguously involved in the same cognitive processes and where EC can be reasonably hypothesized. All four selected ROIs were consistently activated in all subjects across both studied groups. We excluded those brain regions from the DCM analysis that were problematic due to their variable and therefore inconsistent individual ROI coordinates.

The results of the present DCM study confirm the cooperation of the cerebellum, putamen, and SMA during temporal processing and support the previous results of neurophysiological experiments suggesting the existence of links between the BG, cerebellum, and cortex.[28] An estimation of neuronal connection between the DCM areas extends the traditional approaches of fMRI analysis. Consequently, DCM offers a more realistic view of the functioning and the interactions between the neuronal populations. DCM is the first method of EC that models the interaction on a neural level and combines it with a plausible forward neurobiological model (relation between neural activity and BLD signal changes).

Finally, the present study has implications for the neurorehabilitation field. Recent studies have shown that practical rehabilitation techniques (goal management training) for executive impairments in subjects with cerebellar damage or motor imagery training (clinical test battery covering different aspect of motor imagery), can be a useful adjunct to medical management and can help to preserve the patient's functional independence.[37–39] Our research leads to the delineation of other brain areas active during this behavior, and in combination with computer-based neuro-rehabilitation programs, it could improve patient performance and decrease the degree of disability in a manner distinct from pharmacotherapy and based on the neuronal functional interactions.[40–43]

Acknowledgment

This work was supported by the project "CEITEC – Central European Institute of Technology" (CZ.1.05/1.1.00/02.0068) from European Regional Development Fund.

Ovidiu V. Lungu was supported by a pilot project research grant from Québec Network for Research in Aging.

The participation of Jiří Vaníček was supported by the European Regional Development Fund Project FNUSA-ICRC (No.CZ.1.05/1.1.00/02.0123).

References

1. Ivry RB. The representation of temporal information in perception and motor control. *Curr Opin Neurobiol* 1996;6:851-857.
2. Meck WH. Neuropsychology of timing and time perception. *Brain Cogn* 2005;58:1-8.
3. Coull J, Nobre A. Dissociating explicit timing from temporal expectation with fMRI. *Curr Opin Neurobiol* 2008;18:137-144.
4. Meck WH, Penney TB, Pouthas V. Cortico-striatal representation of time in animals and humans. *Curr Opin Neurobiol* 2008;18:145-152.
5. Buhusi CV, Meck WH. What makes us tick? Functional and neural mechanisms of interval timing. *Nat Rev Neurosci* 2005;6:755-765.
6. Wiener M, Turkeltaub P, Coslett HB. The image of time: a voxel-wise meta-analysis. *Neuroimage* 2010;49:1728-1740.
7. Jahanshahi M, Jenkins IH, Brown RG, et al. Self-initiated versus externally triggered movements. I. An investigation using measurement of regional cerebral blood flow with PET and movement-related potentials in normal and Parkinson's disease subjects. *Brain* 1995;118(Pt.4):913-933.
8. Jahanshahi M, Jones CR, Dirnberger G, et al. The substantia nigra pars compacta and temporal processing. *J Neurosci* 2006;26:12266-12273.
9. Tseng YW, Diedrichsen J, Krakauer JW, et al. Sensory prediction errors drive cerebellum-dependent adaptation of reaching. *J Neurophysiol* 2007;98:54-62.
10. O'Boyle DJ, Freeman JS, Cody FW. The accuracy and precision of timing of self-paced, repetitive movements in subjects with Parkinson's disease. *Brain* 1996;119(Pt.1):51-70.
11. Harrington DL, Haaland KY, Hermanowicz N. Temporal processing in the basal ganglia. *Neuropsychology* 1998;12:3-12.
12. Jones CR, Malone TJ, Dirnberger G, et al. Basal ganglia, dopamine and temporal processing: performance on three timing tasks on and off medication in Parkinson's disease. *Brain Cogn* 2008;68:30-41.
13. Jahanshahi M, Jones CR, Zijlmans J, et al. Dopaminergic modulation of striato-frontal connectivity during motor timing in Parkinson's disease. *Brain* 2010;133(Pt.3):727-745.
14. Hoshi E, Tremblay L, Féger J, et al. The cerebellum communicates with the basal ganglia. *Nat Neurosci* 2005;8:1491-1493.
15. Husárová I, Lungu OV, Mareček R, et al. Functional imaging of the cerebellum and basal ganglia during predictive motor timing in early Parkinson's disease. *J Neuroimaging* 2011; Dec 30. doi: 10.1111/j.1552-6569.2011.00663.x. [Epub ahead of print].
16. Galea JM, Bestmann S, Beigi M, et al. Action reprogramming in Parkinson's disease: response to prediction error is modulated by levels of dopamine. *J Neurosci* 2012;32:542-550.
17. Sheth SA, Abuelem T, Gale JT, Eskandar EN. Basal ganglia neurons dynamically facilitate exploration during associative learning. *J Neurosci* 2011;31:4878-4885.
18. Ward CD, Gibb WR. Research diagnostic criteria for Parkinson's disease. *Adv Neurol* 1990;53:245-249.
19. Fahn S, Elton RL, Members of the UPDRS development committee. Unified Parkinson's disease rating scale. In: Fahn S, Marsden CD, Calne DB, Goldstein M, eds. *Recent Developments in Parkinson's Disease.* Florham Park, NJ, USA: Macmillan Healthcare Information, 1987, 153-163.
20. Oldfield RC. The assessment and analysis of handedness: the Edinburgh inventory. *Neuropsychologia* 1971;9:97-113.
21. Bares M, Lungu O, Liu T, et al. Impaired predictive motor timing in patients with cerebellar disorders. *Exp Brain Res* 2007;180:355-365.
22. Bares M, Lungu OV, Husárová I, et al. Predictive motor timing performance dissociates between early diseases of the cerebellum and Parkinson's disease. *Cerebellum* 2010;9:124-135.

23. Kimberley TJ, Birkholz DD, Hancock RA, et al. Reliability of fMRI during a continuous motor task: assessment of analysis techniques. *J Neuroimaging* 2008;18:18-27.
24. Friston KJ, Harrison L, Penny W. Dynamic causal modelling. *Neuroimage* 2003;19:1273-1302.
25. Ethofer T, Anders S, Erb M, et al. Cerebral pathways in processing of affective prosody: a dynamic causal modeling study. *Neuroimage* 2006;30:580-587.
26. Akkal D, Dum RP, Strick PL. Supplementary motor area and presupplementary motor area: targets of basal ganglia and cerebellar output. *J Neurosci* 2007;27:10659-10673.
27. Schell GR, Strick PL. The origin of thalamic inputs to the arcuate premotor and supplementary motor areas. *J Neurosci* 1984;4:539-560.
28. O'Reilly JX, Mesulam MM, Nobre AC. The cerebellum predicts the timing of perceptual events. *J Neurosci* 2008;28:2252-2260.
29. Beudel M, Renken R, Leenders KL, et al. Cerebral representations of space and time. *Neuroimage* 2009;44:1032-1040.
30. Macar F, Coull J, Vidal F. The supplementary motor area in motor and perceptual time processing: fMRI studies. *Cogn Process* 2006;7:89-94.
31. Bostan AC, Strick PL. The cerebellum and basal ganglia are interconnected. *Neuropsychol Rev* 2010;20:261-270.
32. Zhang L, Zhong G, Wu Y, et al. Using Granger-Geweke causality model to evaluate the effective connectivity of primary motor cortex (M1), supplementary motor area (SMA) and cerebellum. *J Biomed Sci Eng* 2010;3:848-860.
33. Mure H, Tang CC, Argyelan M, et al. Improved sequence learning with subthalamic nucleus deep brain stimulation: evidence for treatment-specific network modulation. *J Neurosci* 2012;32:2804-2813.
34. Wearden JH, Smith-Spark JH, Cousins R, et al. Stimulus timing by people with Parkinson's disease. *Brain Cogn* 2008;67:264-279.
35. Artieda J, Pastor MA, Lacruz F, Obeso JA. Temporal discrimination is abnormal in Parkinson's disease. *Brain* 1992;115(Pt.1):199-210.
36. Penny WD, Stephan KE, Mechelli A, et al. Modelling functional integration: a comparison of structural equation and dynamic causal models. *Neuroimage* 2004; 23(Suppl 1):S264-S274.
37. Schweizer TA, Levine B, Rewilak D, et al. Rehabilitation of executive functioning after focal damage to the cerebellum. *Neurorehabil Neural Repair* 2008;22:72-77.
38. Heremans E, Feys P, Nieuwboer A, et al. Motor imagery ability in patients with early- and mid-stage Parkinson disease. *Neurorehabil Neural Repair* 2011;25:168-177.
39. Solodkin A, Peri E, Chen EE, et al. Loss of intrinsic organization of cerebellar networks in spinocerebellar ataxia type 1: correlates with disease severity and duration. *Cerebellum.* 2011; 10:218-232.
40. Hayes SJ, Elliott D, Bennett SJ. General motor representations are developed during action-observation. *Exp Brain Res* 2010;204:199-206.
41. Bares M, Lungu OV, Liu T, et al. The neural substrate of predictive motor timing in spinocerebellar ataxia. *Cerebellum* 2011;10:233-244.
42. Jirenhed DA, Hesslow G. Learning stimulus intervals- adaptive timing of conditioned purkinje cell responses. *Cerebellum* 2011;10:523-535.
43. Jech R, Mueller K, Schroetter ML, Ruzicka E. Levodopa increases functional connectivity in the cerebellum and brainstem in Parkinson´s disease. *Brain* 2013; Jan 30 [Epub ahead of print].

Supporting Information

Additional Supporting Information may be found in the online version of this article at the publisher's website:

Fig S1. (A) The hit ratio as a function of type of movement (constant, accelerating, or decelerating) and the type of speed (fast, medium, or slow) in healthy controls (left panel) and PD subjects (right panel). Within each group, the hit ratio was significantly affected by the type of movement and type of speed, and by their interaction. However, other than a general difference in the hit ratio between the two groups (early PD performance was 90% that of HC group), the kinematic properties of the target affect the hit ratio similarly in both healthy controls and PD subjects. (B) The mean distribution of early errors, late errors, and hits (as percentages of all trials) in both groups. We found significant group differences in the distribution of hits and early errors, but not regarding the late errors. Specifically, the loss in accuracy in the PD group is made at the expense of early errors. (C) The distribution of trial types in the current trial (early errors, hits, late errors) as a function of the stimulus type in the previous trial. The results indicate that the PD group tends to make more early errors in the current trial after making any type of error in the previous trial.